

## Experimental analysis of microstructure and mechanical properties of welded joint of dissimilar alloy AA6082 and AA7075 by TIG and FSW

Jitendra Kumar Maurya<sup>1</sup>, Pawan Kumar<sup>2</sup>

<sup>1</sup>M.Tech Scholar, Department of Mechanical Engineering, Geeta Engineering College, Panipat, India

<sup>2</sup>Assistant Professor, Department of Mechanical Engineering, Geeta Engineering College, Panipat, India

### Abstract

Tungsten inert gas welding is the most commonly used for joining of dissimilar alloy, which are highly recommended in aircraft and automobile engineering. The quality of the weld and strength of the welded joints is higher than the other fusion welding, but there are some unavoidable microstructure defects formation such as porosity and micro cracks is found in the fusion zone. The formation of these defects will result in the reduction of weld strength. On the other hand friction stir welding removes these types of defect and improve the weld quality of dissimilar material.

The present work will focus on the improvement of welded joint of dissimilar material. The friction stir welding destroyed the coarse grains structure in the weld zone and help to dissolves the precipitates of secondary particles, which exist along the grain boundaries. In addition the formation of very fine grain structure was observed in the stir zone as compare to the fusion zone in the TIG welded joint. The ultimate tensile strength of dissimilar alloy (AA6082 and AA7075) increases by increasing the tool rotation. On the welded joints the friction stir welded joint fabricated using tool rotation 1300 rpm have higher tensile stress of 173 MPa with higher 33.5% elongation. The joint efficiency of welded joint with 1300 rpm tool rotation is much higher than the TIG welded joint. Due to grain refinement in friction stir welding the hardness value was found maximum as compare to tungsten inert gas welding. At the high tool rotation speed with same feed rate, welding quality is improved and solve the welding defect like porosity which affect the welded joint. It is found that the residual at the center of the weldment decreases with increases the tool rotational speed. The maximum compressive residual stress 75 MPa was found at TIG weldment, whereas the minimum compressive residual stress 36 MPa was found at the center of the weldment having tool rotation speed 1300 rpm.

©2019 ijrei.com. All rights reserved

### 1. Introduction

It is a solid-state joining technology which has been used to successfully weld aluminum and its alloys. FSW is performed with a non-consumable rotating tool consisting of a smaller diameter pin and larger diameter shoulder. The forces generated during FSW are significant; and a proper fixture design is critical to the success of the weld. The working principle of FSW process is schematically represented in the Fig. 3. Friction stir weld can be accomplished in any position. [1-3]. The ultimate tensile strength and hardness of bimetallic weld joint increases by increasing the pre-stress, and ductility was decreases when thermal loading increases. The tool contacts and penetrates into the abutting edges of the sheets being joined and traverses along the faying interface of the joint. While the tool rotates, it generates a large amount of frictional heat on the work piece.

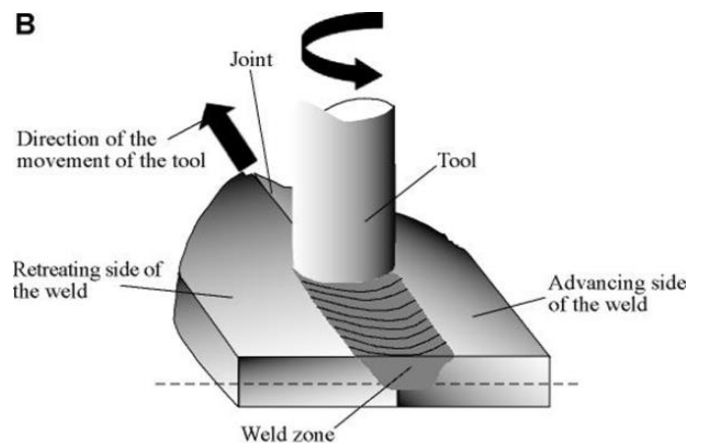


Figure 1: Friction Stir Welding

This heat softens the material surrounding the pin and facilitates movement of material flow around the pin to displace material from the front of pin to the backside of the rotating pin. Since no melting occurs in this process, the process was patented as a solid-state joining technology. The center of the joint, the weld nugget, namely, stir zone (SZ), exhibits a size and morphology which depends on the size and geometry of the tool involved. In terms of the weld nugget microstructure, it is grouped into three features of the adjacent space, consisting of the stir zone, thermo-mechanically affected zone (TMAZ), and heat affected zone (HAZ). The stir zone (also known as the dynamically

recrystallized zone) is a region of heavily deformed material that roughly corresponds to the location of the pin during welding. The grains within the stir zone are roughly equiaxed and often an order of magnitude smaller than the grains in the parent material. The tensile strength of the joint is lower than that of the parent metal and it is directly proportional to the travel/ welding speed. Welding parameter such as tool rotation, transverse speed and axial force have a significant effect on the amount of heat generated and strength of FSW joints [4-8]. The following conclusion has been made from the literature review which are as below.

Author	Title of Paper	Material	Input Parameter	Conclusions
Aonuma. M., et al [9]	Dissimilar metal joining of ZK60 magnesium alloy and titanium by friction stir welding	Titanium and MgZnZr alloy Thickness - 2.0 mm	<ul style="list-style-type: none"> <li>➤ Tool shoulder diameter 15mm.</li> <li>➤ Pin diameter 6 mm.</li> <li>➤ Tool pin length 1.9mm</li> <li>➤ Tool rotational speed 850 rpm</li> <li>➤ Tool traverse speed 50, 100 mm/min</li> <li>➤ Tilt angle 3°</li> <li>➤ Probe offsets of 1.0 and 1.5 mm</li> </ul>	<ul style="list-style-type: none"> <li>➤ Alloying elements of ZK60 Mg–Zn–Zr alloy on the microstructure of the dissimilar joint interface with titanium and the joint strength in comparison with pure magnesium and titanium has been investigated.</li> <li>➤ The fracture of the joint by tensile test occurred mainly in the stir zone of Mg–Zn–Zr alloy and partly at the joint interface. The tensile strength of the Mg–Zn–Zr alloy and titanium joint was higher than that of the pure magnesium and titanium.</li> </ul>
Chen.Y. C., et al [10]	Microstructural characterization and mechanical properties in friction stir welding of aluminum and titanium dissimilar alloys	ADC12 cast aluminum alloy sheet & Pure titanium sheet	<ul style="list-style-type: none"> <li>➤ Tool shoulder and pin diameter are 15 &amp; 5 mm.</li> <li>➤ Tool pin length 3.9</li> <li>➤ Tool rotational speed 850 rpm.</li> <li>➤ Tool traverse speed 50 and 100 mm/min.</li> <li>➤ Tilt angle 3 °</li> </ul>	<ul style="list-style-type: none"> <li>➤ ADC12 Al alloy and pure Ti can be successfully lap welded using friction stir welding technology.</li> <li>➤ The maximum failure load of lap joints can reach 62% that of ADC12 Al alloy base metal. The transient phase TiAl3 forms at the joining interface by Al–Ti diffusion reaction.</li> </ul>
Liu.H.J., et al [11]	Microstructural characteristics and mechanical properties of friction stir welded joints of Ti–6Al–4V titanium alloy	Ti6Al 4V plates Thickness - 2 mm	<ul style="list-style-type: none"> <li>➤ Tool rotational speed 400 rpm.</li> <li>➤ Tool traverse speed 25, 50 and 100 mm/min.</li> <li>➤ Tilt angle 2.5.</li> <li>➤ Plunge depth 0.2 mm</li> </ul>	<ul style="list-style-type: none"> <li>➤ Defect-free welds were successfully obtained with welding speeds ranging from 25 to 100 mm/min.</li> <li>➤ A bimodal microstructure was developed in the stir zone during friction stir welding, while microstructure in the heat affected zone was almost not changed compared with the base material.</li> </ul>
Bang.H., et al [12]	Joint properties of dissimilar Al6061-T6 aluminum alloy/Ti–6%Al–4%V titanium alloy by gas tungsten arc welding assisted hybrid friction stir welding	Al6061-T6 aluminum alloy and Ti6%Al4%V titanium alloy Thickness - 3.5 mm	<ul style="list-style-type: none"> <li>➤ Tool shoulder and pin diameter 18 &amp; 5 mm.</li> <li>➤ Tool pin length 3.3 mm</li> <li>➤ Tool rotational speed 850 rpm.</li> <li>➤ Tool traverse speed 50, 100 mm/min.</li> <li>➤ Tilt angle 3°</li> <li>➤ Probe off sets of 2 mm</li> </ul>	<ul style="list-style-type: none"> <li>➤ The ultimate tensile strength was approximately 91% in HFSW welds by that of the Al alloy base metal, which was 24% higher than that of FSW welds without GTAW under same welding condition.</li> <li>➤ It was found that elongation in FSW welds increased significantly compared with that of FSW welds, which resulted in improved joint strength. The ductile fracture was the main fracture mode in tensile test of HFSW welds.</li> </ul>

Zhang, H.W., et al [13]	3D modeling of material flow in friction stir welding under different process parameters.	AA 6061 -T6	<ul style="list-style-type: none"> <li>➤ Tool rotation speed, welding speed and axial force</li> </ul>	<ul style="list-style-type: none"> <li>➤ It seems that there is a quasi-linear relation between the change of the axial load on the shoulder and the variation of the equivalent plastic strain. The material flow can be accelerated with the increase of the translational and angular velocity.</li> </ul>
Zhang, H., Lin,S.B., [14]	Defects formation procedure and mathematic model for defect free friction stir welding of magnesium alloy	AZ31 Magnesium alloy	<ul style="list-style-type: none"> <li>➤ Welding speed and welding rate</li> </ul>	<ul style="list-style-type: none"> <li>➤ The pore firstly occurred near the welding line at relatively low welding speed, but move into advancing side and up part of the weld when continues to increase the welding speed.</li> </ul>
Dressler. U., et al [15]	Friction stir welding of titanium alloy TiAl6V4 to aluminium alloy AA2024-T3	TiAl6V4 and Al-alloy 2024-T3 Thickness 2 mm	<ul style="list-style-type: none"> <li>➤ Tool concave shoulder diameter 18 mm.</li> <li>➤ Pin threaded and tapered diameter 6 mm</li> <li>➤ Tool pin length 5.7mm.</li> <li>➤ Tool rotational speed 800 rpm.</li> <li>➤ Tool traverse speed 100 mm/min</li> <li>➤ Tilt angle 2.5 °</li> </ul>	<ul style="list-style-type: none"> <li>➤ Hardness and tensile strength of the butt joint were investigated.</li> <li>➤ The weld nugget exhibits a mixture of fine recrystallized grains of aluminium alloy and titanium particles.</li> <li>➤ Hardness profile reveals a sharp decrease at titanium/aluminium interface and evidence of microstructural changes due to welding on the aluminium side. The ultimate tensile strength of the joint reached 73% of A2024-T3 base material strength.</li> </ul>
Mironov. S., et al [16]	Development of grain structure during friction stir welding of pure titanium	Purity a-titanium (ASTM Grade, Thickness- 3 mm thick Butt-welded Joint	<ul style="list-style-type: none"> <li>➤ Tool convex shoulder diameter 15 mm.</li> <li>➤ Pin threaded and tapered diameter 5.1 mm.</li> <li>➤ Tool tapered pin length 3 mm.</li> <li>➤ Tool rotational speed 200 rpm</li> </ul>	<ul style="list-style-type: none"> <li>➤ The global straining state during the process was deduced to be close to the simple shear with the shear surface being nearly along the truncated cone having a diameter close to that of the tool shoulder in the top part of the SZ.</li> <li>➤ The grain structure evolution was shown to be a complex process driven mainly by the texture-induced grain convergence, but also involving the geometrical effects of strain and limited discontinuous recrystallization.</li> </ul>
Arora.A., et al [17]	Toward optimum friction stir welding tool shoulder diameter	AA6061 alloy	<ul style="list-style-type: none"> <li>➤ Shoulder diameter 15, 18, 21 mm, Pin diameter 6 mm., Pin length 5.5 mm., Pin profile Cylindrical, no thread, Tool Rotational velocity 900-1500 rpm</li> </ul>	<ul style="list-style-type: none"> <li>➤ The optimum tool shoulder diameter computed from this principle using a numerical heat transfer and material flow model resulted in best weld metal strength in independent tests and peak temperatures that are well within the commonly encountered range.</li> </ul>
Baillie.P. [18]	Friction Stir Welding of 6mm thick carbon steel underwater and in air	S275 hot rolled structural steel	<ul style="list-style-type: none"> <li>➤ Travel speed 100 (mm/min), Speed of rotation 200 revs/min).</li> <li>➤ FSW Travel speed 100 (mm/min) Speed of rotation 240 (revs/min)</li> </ul>	<ul style="list-style-type: none"> <li>➤ Between the processes the longitudinal tensile results are the same, the micro hardness does not vary. It was also shown that underwater FSW has benefits compared to SAW and FSW in air. Charpy impact toughness was however shown to decrease for the underwater weld. Within the available data it is difficult to fully explain the toughness difference as the relative grain sizes do not vary significantly.</li> </ul>

Panneerselvam.K., et al [19]	Study on friction stir welding of nylon 6 plates	Nylon 6 Thickness - 10mm	<ul style="list-style-type: none"> <li>➤ Tool shoulder dia 24 mm, Pin dia 6 mm, Tool pin length 9.5 mm, Tool rotating speed (rpm) 750 to 4000, Welding Feeds 10- 100 mm/min.</li> </ul>	<ul style="list-style-type: none"> <li>➤ By using secondary heat sources with 0.5 or 0.6mm gap provision in between shoulder and top of the workpiece is the optimal gap to weld the nylon 6 material without any visible defects. When fixed welding speed in between 600 and 1200 rpm and feed rate also in between 10 and 40mm/min, got good weld region compared with the other.</li> </ul>
Sato.Y.S., et al [20]	Evaluation of microstructure and properties in friction stir welded super austenitic stainless steel	NSSC 270 superaustenitic stainless steel thickness - 6 mm	<ul style="list-style-type: none"> <li>➤ Rotational speed 400 and 800 rev per min,</li> <li>➤ Traverse speed 1 and 0.5 mm /s</li> </ul>	<ul style="list-style-type: none"> <li>➤ Findings of the present study suggest that low heat input friction stir welding is an effective method to produce a weld with relatively good properties in super austenitic stainless steels.</li> <li>➤ The high rotational speed drastically reduced mechanical and corrosion properties of the weld due to the high density of intermetallic phases, while the reduction of the properties was not significant at low rotational speed.</li> </ul>
Ramesh.R., et al [21]	Microstructure and mechanical characterization of friction stir welded high strength low alloy steels	High strength low alloy HSLA plates thickness - 3 mm	<ul style="list-style-type: none"> <li>➤ Tool shoulder diameter 18 mm. Tool pin length 2.7 mm. Pin profile was tapered cylindrical with a dia 8 mm) Traverse speed 57, 67, 77, 87 mm/min</li> </ul>	<ul style="list-style-type: none"> <li>➤ The joint strength was 540 MPa at 57 mm/min and 407 MPa at 97 mm/min. The higher strength below 78 mm/min traverse speed was due to hard weld nugget. The lower joint strength with further increase in traverse speed was due to poor consolidation and macroscopic defects. The tendency to form macroscopic defects increased with increase in traverse speed. Root flaw and groove defect were observed at a traverse speed of 97 mm/min.</li> </ul>
Gan.W., et al [22]	Tool materials selection for friction stir welding of L80 steel	High strength pipe steel L80	<ul style="list-style-type: none"> <li>➤ Tool Travel speed 1.7 mm/s. Tool Rotational speed 170 rev/min, Pin length 1.5 mm</li> </ul>	<ul style="list-style-type: none"> <li>➤ The results indicate that the physical wear amounts to a material loss of 7% of the original volume. Mushrooming of the tool was successfully predicted. The calculations also indicated that the pin tool material should have a yield strength larger than 400 MPa.</li> </ul>

## 2. Experimental method and material

### 2.1 Tungsten Inert gas welding

Manual tungsten argon arc welding is generally considered to be the most difficult of all welding processes commonly used in the industry. Because the welder must maintain a short arc, the length of the electrode, and requires great care and skill to prevent contact between the workpieces. The torch is similar to welding, GTAW, which usually requires two hands, because for most applications, the welder is manual, and on the other hand increases the torch to the filler metal into the weld zone. To strike the welding arc, similar to a high frequency generator (Tesla coil) is to provide an electrical spark; this spark is used to conduct a conductive path through the shielding gas and allows rotation of the electrode and the working split piece The arc, except for the usual 1.53 mm (0.06-0.12 in).

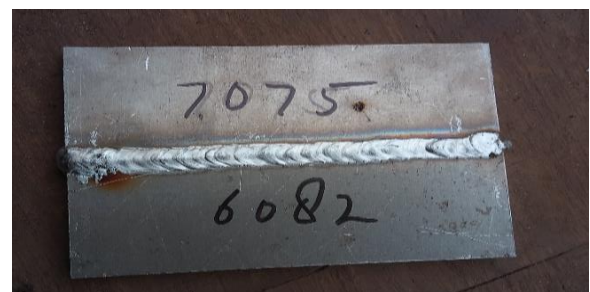


Figure 2: Tungsten inert gas welding

### 2.2 Friction stir welding

The experiments have been carried out on the friction stir welding machine with necessary equipment details such as tool, process parameter and safety precautions. Process parameter involved

here is the tool rotation speed, welding speed, tilt angle and tool geometry. the FSP tool geometry, aluminum alloy plates, friction stir welding machine, processed zone and various tool manufactured to perform the desired experiments. The process of FSP begins with the tool design and fabrication. The main and the crucial thing of this work were the tool design for friction stir processing process, which would fix in the available friction stir welding machine shank. Initially FSP tool designed in such a way that the tool geometry was very simple with cylindrical tool, shank dia-25 mm, shoulder dia-20 mm, pin dia-8 mm, pin lenth-5.5 mm.



Figure 3: Friction stir welding

### 2.3 Chemical composition of Al- alloy

Aluminium alloy of AA6082 and AA7075 are selected to fabricate dissimilar joints using TIG and friction stir welding (FSW). The length, width and thickness of both the alloy plates are chosen as 120, 40 and 6.3 mm respectively. The chemical composition of AA6082 and AA7075 are given in table 1.

Table 1: Chemical composition of Aluminum alloy

Al- Alloy	Si	Fe	Cu	Mn	Mg	Cr	Zn	Ti	Al
6082	1.3	0.52	0.1	0.5	0.8	0.15	0.2	0.2	Balance
7075	0.05	0.1	1.3	.03	2.7	0.2	5.78	0.06	Balance

### 2.4 Specimen Dimensions

Tensile testing was performed on ASTM E8 standard samples to evaluate the mechanical properties of different welds. In all cases, the failure occurred in the original metal of AA 6082. Before the fracture, Welds produced a large amount of plastic deformation in the ductile failure mode.

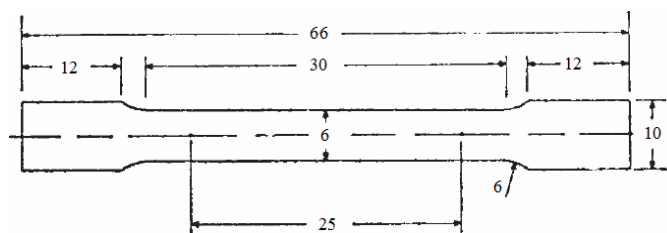


Figure 1: ASTM E8 standard sub tensile specimen

### 2.5 Processing Parameter

The Processing parameter for Tungsten inert gas welding and friction stir welding were chosen by trial and error attempts until no visually detected defect could be identified. The penetration depth was adapted to fully penetrated butt joint in a material of 5.5 mm thickness.

Table 2: Processing parameter for TIG welding

Type	Current (A)	Voltage (V)	Wire feed (cm/min)
TIG Welding	150	12	3.5

Table 3: Processing parameter for TIG welding

Sample No	Current (amp)	Welding Speed (mm/min)	Tool rotational speed (rpm)	Frequency (HZ)
1	6.5	44	1000	31.25
2			1100	32.96
3			1200	34.12
4			1300	37051

## 3. Results and Discussions

### 3.1 Tensile strength

Friction stir welding may be used to join a different member of material. Defect free welds with excellent mechanical properties can be achieved by FSW. The stress strain curves for TIG and FSW joints is shown in figure 18. The tensile properties like ultimate tensile strength and % elongation of the weldments are presented in table 3. The ultimate tensile strength and hardness of dissimilar alloy (AA6082 and AA7075) increases by increasing the tool rotation as shown in figure. On the welded joints the friction stir welded joint fabricated using tool rotation 1300 rpm have higher tensile stress of 173 MPa with higher 33.5% elongation. The joint efficiency of welded joint with 1300 rpm tool rotation is much higher than the TIG welded joint.

### 3.2 Tool rotation speed and welding speed

Processing parameters of friction stir welding are the main factor affecting the welded joint. If the rotating speed of FSW tool is too low then the frictional heat will not generated enough to induce plasticized flow which lead to defect in the weldment. The other important factor is welding speed. When welding speed is too low then the frictional heat makes the temperature too high then there is the possibility of excess heat flow in the welded joint, whereas when the weld speed increases the material just below the tool softens to such a degree that it act as a lubricant, lowering the friction and reduce the temperature.

Table 4: Mechanical Properties of welded joint

Welding	Average Stress (MPa)	Average Strain (%)
TIG welding	144	19.9
FSW with 1000 rpm	149.1	23
FSW with 1100 rpm	153.03	26.1
FSW with 1200 rpm	168.1	31.7
FSW with 1300 rpm	173	33

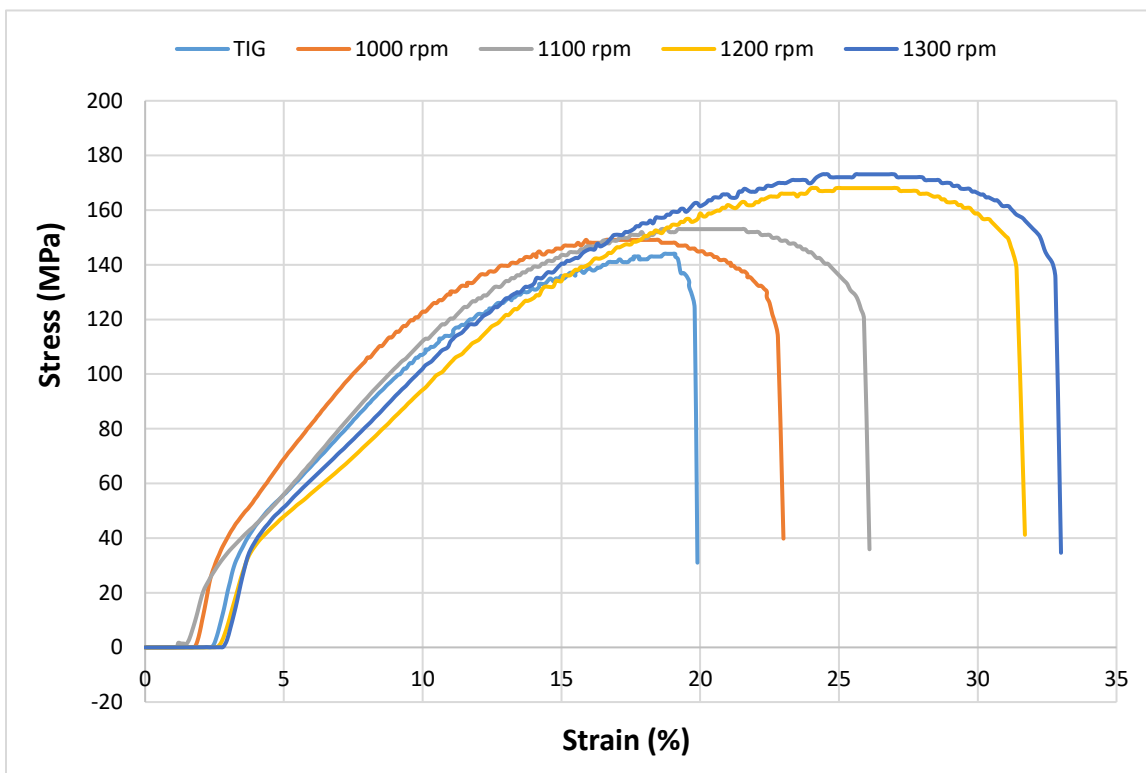


Figure 2: Stress strain diagram for TIG and FSW joint

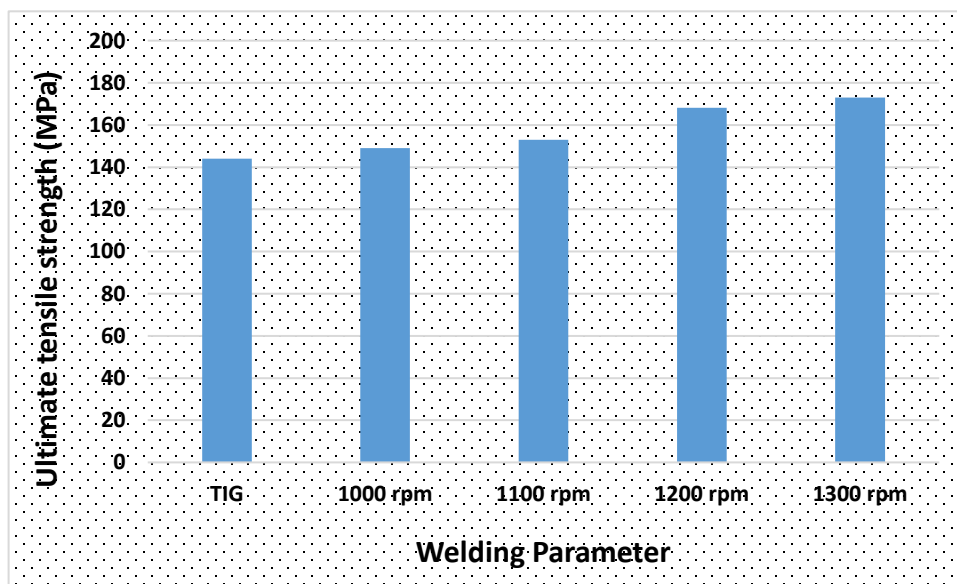


Figure 3: Comparison of tensile stress of TIG and FSW weldment

### 3.3 Residual Stress analysis

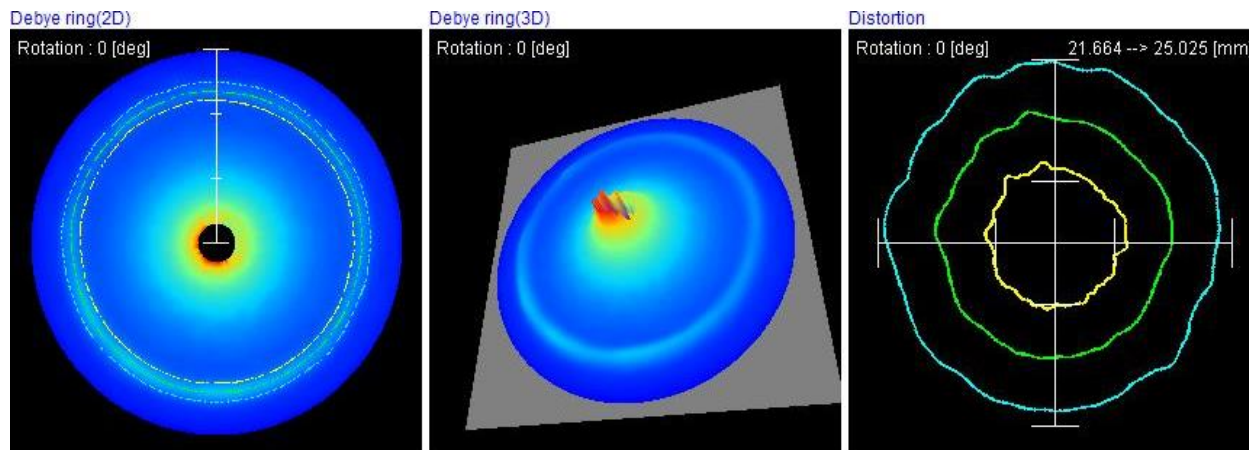
It is found that in the region where the equivalent plastic strain increases, the residual stress is decreases. When away from the stir zone point of the welded joint, the residual stress is slightly increases but after stir zone the distribution of residual stress remains almost steady. Because of unsymmetrical deformation at the welding zone, the residual stresses are not symmetric to the welding line. When the fixture are released and the temperature

is going to reduce to room temperature then the material in the nugget zone tends to recover. But the weldment in the HAZ has smaller deformation and will prevent the recovery process in the nugget zone. So the maximum residual stress (RS) occur in the boundaries of the heat affected zone (HAZ) and minimum in the nugget zone (NZ).

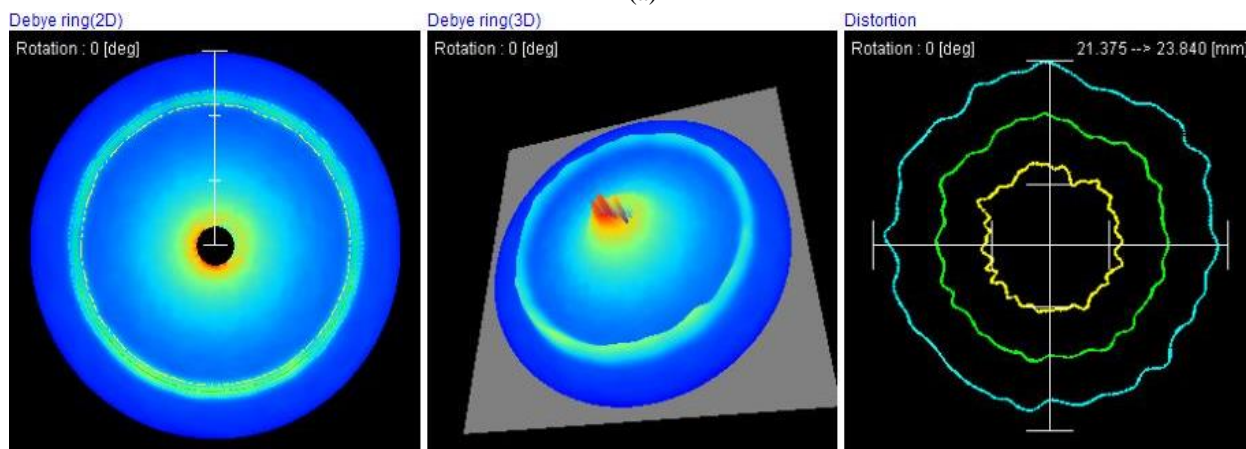
There are two types of residual stress distribution found in the weldment, usually tensile residual stress located in the weld area, whereas compressive residual stress can be found at heat affected

zone. The results are obtained by the computational method as shown in fig. 21 for the five specimen with different processing parameters at the center of the weldment. It is found that the residual at the center of the weldment decreases with increases the tool rotational speed. The maximum compressive residual

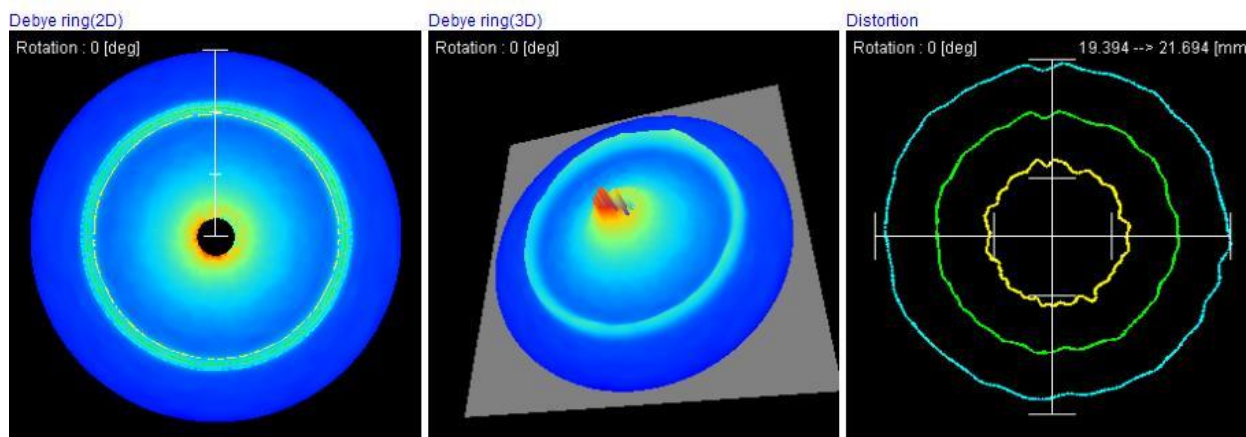
stress 75 MPa was found at TIG weldment, whereas the minimum compressive residual stress 36 MPa was found at the center of the weldment having tool rotation speed 1300 rpm as shown in fig. 22.



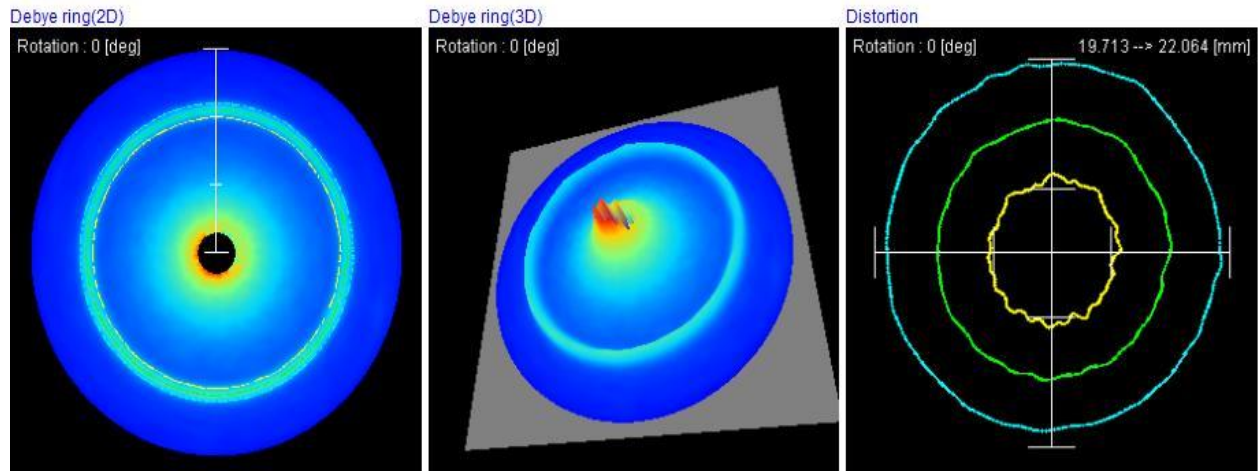
(a)



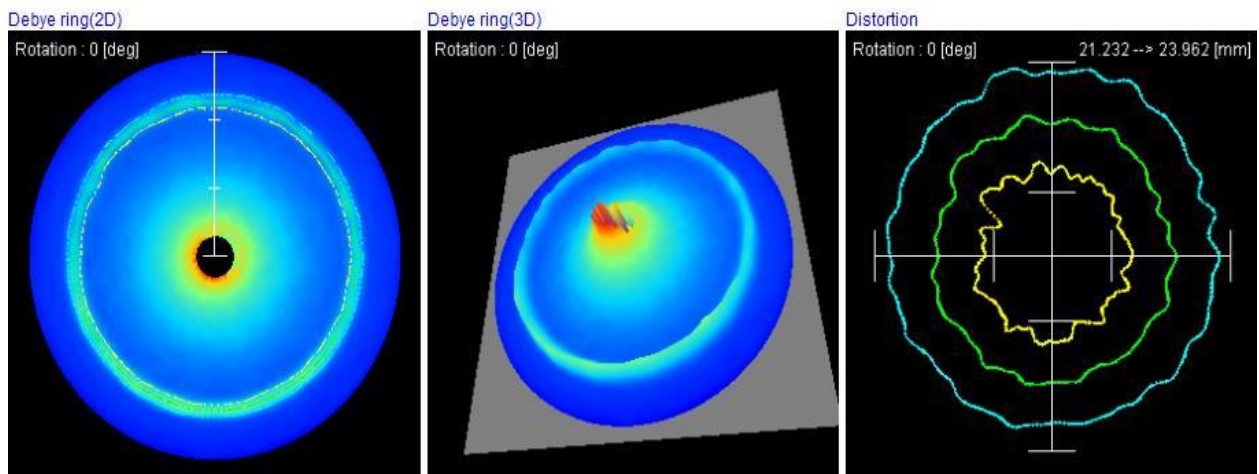
(b)



(c)



(d)



(e)

Figure 4: The residual stress distribution and distortion ring at the center of the weldment, (a) TIG welded joint, (b) 1000 rpm, (c) 1100 rpm, (d), 1200 rpm, (e) 1300 rpm

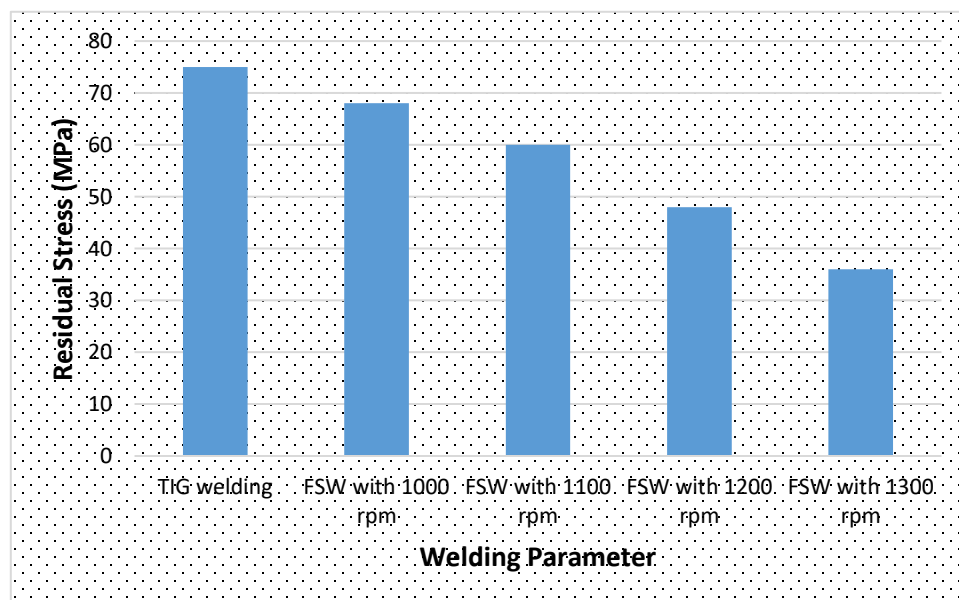


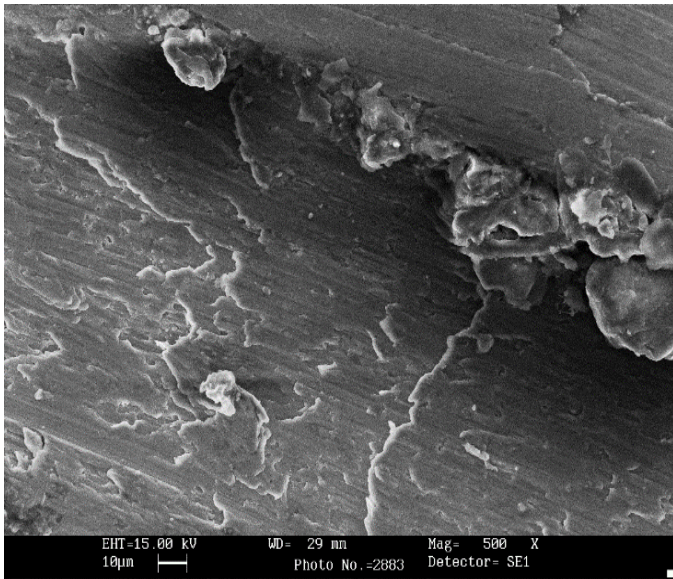
Figure 5: Comparison of residual stress for different weldment

### 3.4 Microstructure Analysis

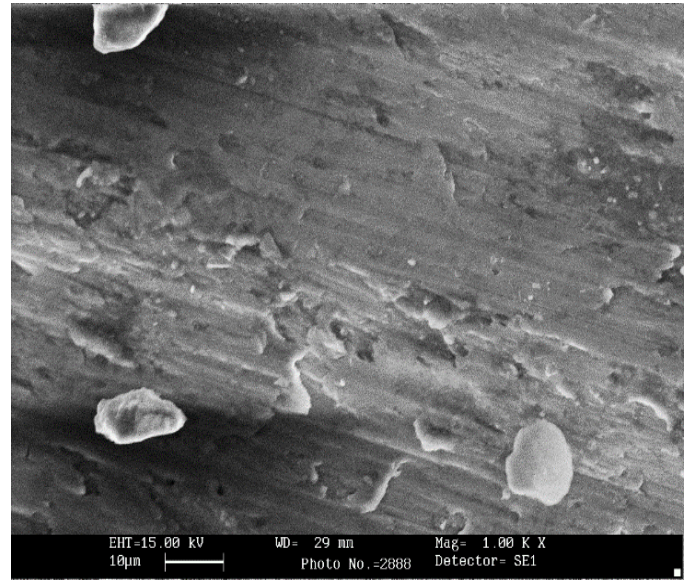
The pin influenced region in the friction stir welding is defined as the bottom portion of stir region, which experiences the effects like heat generation and material flow, which are solely created by the rotation and rubbing of the tool pin during friction stir welding. The strength of dissimilar alloy mainly concern on the mechanical interlocking of the material, thus the material should be flowed and mixed properly, so the dissimilar material flow decide the formation of defect free stir zone and strength of the dissimilar joint. Fig.22 (b-e) shows the microstructure of welded

joint of AA6082 and AA7075 of the nugget zone of the joint interface of the weld produced tool rotation speed of 1000-1300 rpm with 44 mm/min transvers speed. The microstructure shows good stirring and more consolidate between AA6082 and AA7075 which improve the weld quality of the weldment. TIG welded joint influenced region shows larger grain size than the friction stir welded joint.

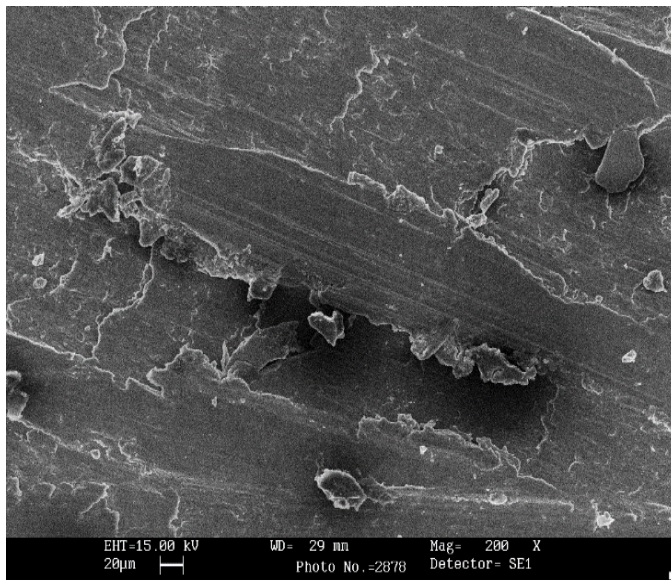
Additionally, most grain in heat affected zone contained a high dislocation density with a network structure as shown in fig. 22(a), suggested that recovery has not been completed or was continuous in nature. Likewise, dislocations of particles were also observed in stir zone as shown in fig.22 (b-e).



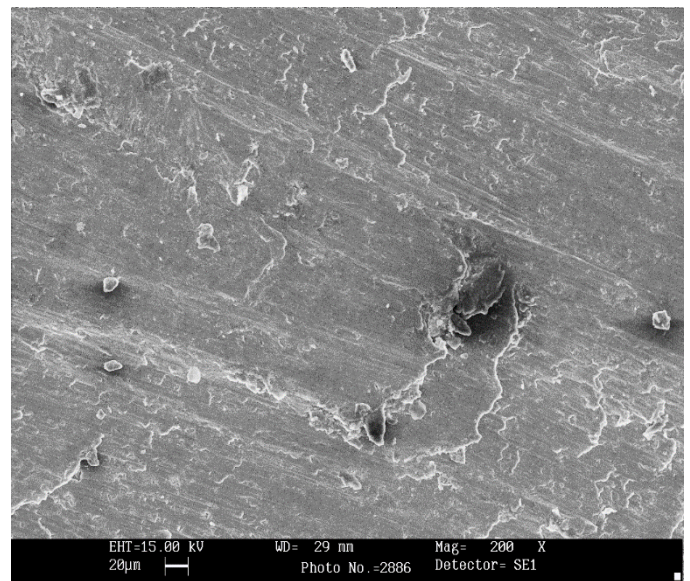
(a)



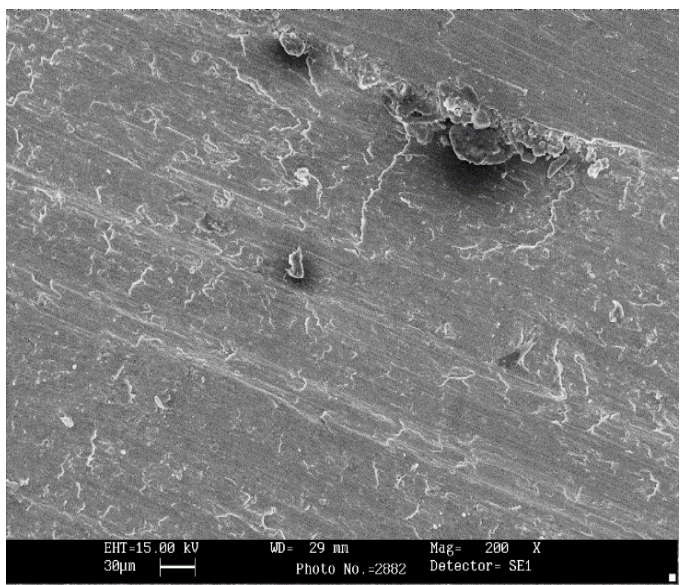
(b)



(c)



(d)



(e)

Figure 6: SEM images of transverse cross section, (a) TIG welded joint, (b) at 1000 rpm, (c) at 1100 rpm, (d) at 1200 rpm, (e) at 1300 rpm

### 3.5 Microhardness

The graphical representation of microhardness of welded joint with different processing parameter as shown in fig. 23. The microhardness values are less momentous in affecting the mechanical properties of the welded joint, because processing parameter (tool rotation speed, current, feed rate etc.) have more influencing factor over the hardness value [64]. The microhardness values at the middle and bottom of the welded

joint detected the major effect, because the grain size and microhardness number were changed due to solidification sequence and cooling rate of the weldment. The microhardness number also play a very important role to recognizing the metallurgical phase. The highest micro-hardness was found at the center of the welded joint in friction stir welding at 1300 rpm with feed rate 44 mm/min and the lowest micro-hardness was found at the center of TIG welded joint as shown in fig. 23.

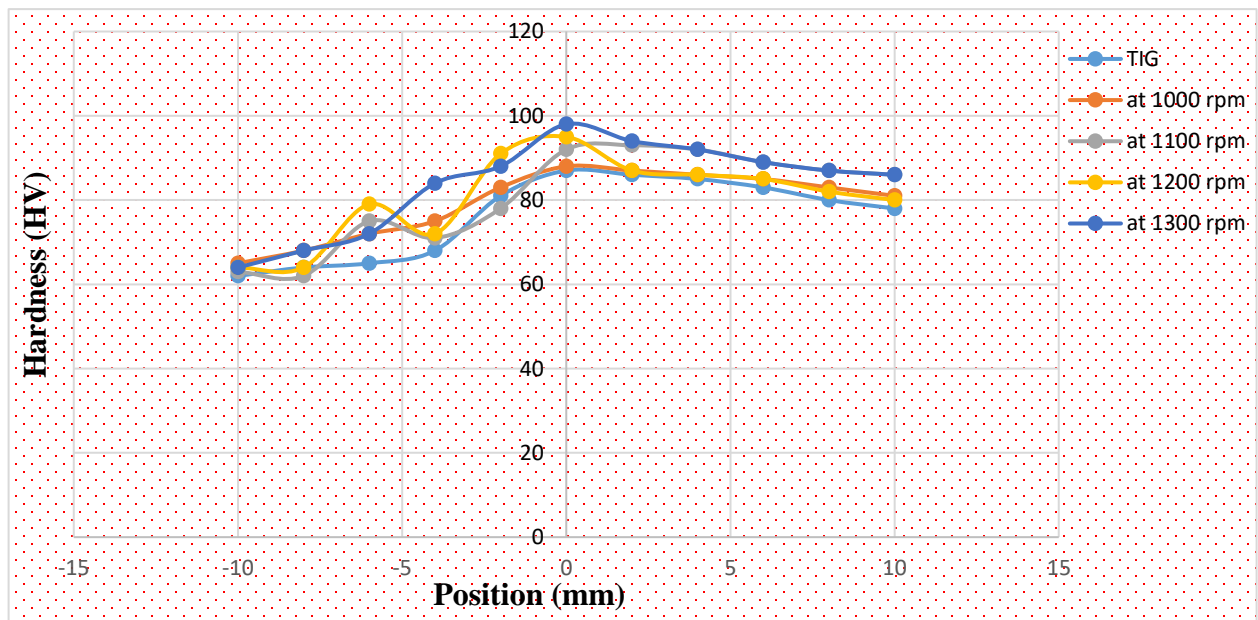


Figure 7: Comparison of microhardness of different processing parameter

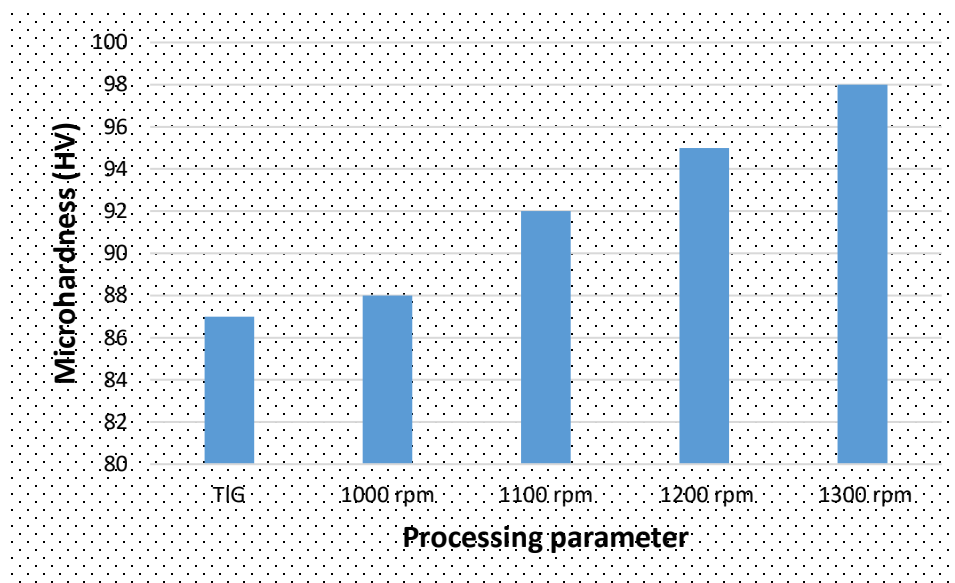


Figure 8: Comparison of microhardness of welded joint

#### 4. Conclusions

Experimental analysis of microstructure and mechanical properties of welded joint (TIG and FSW) of dissimilar alloy AA6082 and AA7075 with different processing parameter has been done, and the following conclusion can be made.

- The ultimate tensile strength of dissimilar alloy (AA6082 and AA7075) increases by increasing the tool rotation. On the welded joints the friction stir welded joint fabricated using tool rotation 1300 rpm have higher tensile stress of 173 MPa with higher 33.5% elongation. The joint efficiency of welded joint with 1300 rpm tool rotation is much higher than the TIG welded joint.
- Due to grain refinement in friction stir welding the hardness value was found maximum as compare to tungsten inert gas welding.
- At the high tool rotation speed with same feed rate, welding quality is improved and solve the welding defect like porosity which affect the welded joint.
- It is found that the residual at the center of the weldment decreases with increases the tool rotational speed. The maximum compressive residual stress 75 MPa was found at TIG weldment, whereas the minimum compressive residual stress 36 MPa was found at the center of the weldment having tool rotation speed 1300 rpm.

#### References

[1] Yutaka SS, Hiroyuki K. Microstructural evolution of 6063, aluminum during friction stir welding. *Metall Mater Trans A* 1999;30A:2429–37.  
 [2] Liu G, Murr LE. Microstructural aspects of the friction-stir welding of 6061-T6 aluminum. *Scripta Mater* 1997;37(3): 355–61.  
 [3] Yutaka SS et al. Microstructural factors governing hardness in friction-stir welds of solid-solution-hardened Al alloys. *Metall Mater Trans* 2001;32A:3033–41.

[4] Husain Mehdi, R.S. Mishra, Mechanical properties and microstructure studies in Friction Stir Welding (FSW) joints of dissimilar alloy- A Review, *Journal of Achievements in Materials and Manufacturing Engineering* 77/1 (2016) 31-40.  
 [5] Husain Mehdi, R.S. Mishra, Influences of Process Parameter and Microstructural Studies in Friction Stir Welding of Different Alloys: A Review, *International Journal of Advanced Production and Industrial Engineering, IJAPIE-SI-MM* 509 (2017) 55–62.  
 [6] Husain Mehdi, Shwetanshu Gaurav, Teetu Kumar, Prasoon Sharma, Mechanical Characterization of SA508Gr3 and SS-304L Steel Weldments, *International Journal of Advanced Production and Industrial Engineering, Vol-2, Issue-1*, 41-46.  
 [7] Husain Mehdi, R.S. Mishra, Mechanical and microstructure characterization of friction stir welding for dissimilar alloy- A Review, *International Journal of Research in Engineering and Innovation*, vol-1, Issue-5 (2017), 57-67.  
 [8] Husain Mehdi, R.S. Mishra, Analysis of Material Flow and Heat Transfer in Reverse Dual Rotation Friction Stir Welding: A Review, *International Journal of Steel Structures*, Vol.19, Issue 2 (2019), pp 422–434.  
 [9] Aonuma, M., & Nakata, K. (2012). Dissimilar metal joining of ZK60 magnesium alloy and titanium by friction stir welding. *Materials Science & Engineering B*, 177(7), 543–548.  
 [10] Chen, Y. C., & Nakata, K. (2009). Microstructural characterization and mechanical properties in friction stir welding of aluminum and titanium dissimilar alloys. *Materials and Design*, 30(3), 469–474.  
 [11] Liu, H. J., Zhou, L., & Liu, Q. W. (2010). Microstructural characteristics and mechanical properties of friction stir welded joints of Ti – 6Al – 4V titanium alloy. *Materials and Design*, 31(3), 1650–1655.  
 [12] Bang, H., Bang, H., Song, H., & Joo, S. (2013). Joint properties of dissimilar Al6061-T6 aluminum alloy / Ti – 6 % Al – 4 % V titanium alloy by gas tungsten arc welding assisted hybrid friction stir welding. *Materials and Design*, 51, 544–551.  
 [13] H.W. Zhang , Z. Zhang, J.T. Chen, 3D modeling of material flow in friction stir welding under different process parameters, *Journal of Materials Processing Technology*, 183, (2007), 62–70.  
 [14] H. Zhang , S.B. Lin, L. Wu, J.C. Feng, S.L. Ma, Defects formation procedure and mathematic model for defect free friction stir welding of magnesium alloy, *Materials and Design* ,27, (2006) ,805–809.  
 [15] Dressler, U., Biallas, G., & Mercado, U. A. (2009). Friction stir welding of titanium alloy TiAl6V4 to aluminum alloy AA2024-T3, 526, 113–117.  
 [16] Mironov, S., Sato, Y. S., & Kokawa, H. (2009). Development of grain structure during friction stir welding of pure titanium. *Acta Materialia*, 57(15), 4519–4528.

- [17] Arora, A., De, A., & Debroy, T. (2011). Toward optimum friction stir welding tool shoulder diameter, 64, 9–12.
- [18] Baillie, P., Campbell, S. W., Galloway, A. M., Cater, S. R., & Mcpherson, N. A. (n.d.). Friction Stir Welding of 6mm thick carbon steel underwater and in air .
- [19] Panneerselvam, K., & Lenin, K. (2013). Study on friction stir welding of nylon 6 plates, 1, 116–120.
- [20] Sato, Y. S., Harayama, N., Kokawa, H., Inoue, H., Tadokoro, Y., Tsuge, S., Tsuge, S. (2017). Evaluation of microstructure and properties in friction stir welded superaustenitic stainless steel Evaluation of microstructure and properties in friction stir welded superaustenitic stainless steel, 1718(May).
- [21] Ramesh, R., Dinaharan, I., Kumar, R., & Akinlabi, E. T. (2017). Materials Science & Engineering A Microstructure and mechanical characterization of friction stir welded high strength low alloy steels. Materials Science & Engineering A, 687(November 2016), 39–46.
- [22] Gan, W., Li, Z. T., Khurana, S., Gan, W., Li, Z. T., & Khurana, S. (2017). Tool materials selection for friction stir welding of Tool materials selection for friction stir welding of L80 steel, 1718(May).

**Cite this article as:** Jitendra Kumar Maurya, Pawan Kumar, Experimental analysis of microstructure and mechanical properties of welded joint of dissimilar alloy AA6082 and AA7075 by TIG and FSW, International Journal of Research in Engineering and Innovation Vol-3, Issue-4 (2019), 253-264.